TELEVISION OBSERVATIONS OF MERCURY BY MARINER 10

BRUCE C. MURRAY, MICHAEL J. S. BELTON, G. EDWARD DANIELSON,
MERTON E. DAVIES, DONALD GAULT, BRUCE HAPKE, BRIAN O'LEARY,
ROBERT G. STROM, VERNER SUOMI AND NEWELL TRASK

206

A Preprint of a Manuscript from

THE PROCEEDINGS OF THE SOVIET-AMERICAN CONFERENCE ON THE COSMOCHEMISTRY OF THE MOON AND PLANETS

HELD IN MOSCOW, USSR, ON JUNE 4–8, 1974

Distributed by

THE LUNAR SCIENCE INSTITUTE

HOUSTON, TEXAS 77058

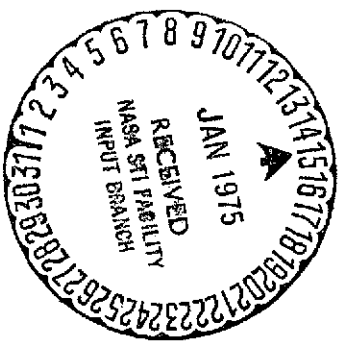

TO MAKE THE INFORMATION CONTAINED HEREIN AS WIDELY AND AS RAPIDLY AVAILABLE TO THE SCIENTIFIC COMMUNITY AS POSSIBLE. NASA EXPECTS TO PUBLISH THE ENGLISH-LANGUAGE VERSION OF THE PROCEEDINGS IN LATE 1975. THE FINAL TEXT MAY INCLUDE MINOR EDITORIAL CHANGES IN FORMAT, etc.

JOHN H. POMEROY, NASA HEADQUARTERS
TECHNICAL EDITOR

MERCURY'S SURFACE:

PRELIMINARY DESCRIPTION AND INTERPRETATION FROM MARINER 10 PICTURES

by

BRUCE C. MURRAY
California Institute of Technology
Pasadena, California 91109

BRUCE HAPKE
University of Pittsburgh
Pittsburgh, Pennsylvania 15260

MICHAEL J. S. BELTON
Kitt Peak National Observatory
Tucson, Arizona 85726

BRIAN O'LEARY
Hampshire College
Amherst, Massachusetts 01002

G. EDWARD DANIELSON
Jet Propulsion Laboratory
Pasadena, California 91103

ROBERT G. STROM
University of Arizona
Tucson, Arizona 85726

MERTON E. DAVIES
Rand Corporation
Santa Monica, California 90401

VERNER SUOMI
University of Wisconsin
Madison, Wisconsin 53706

DONALD E. GAULT
Ames Research Center
Moffett Field, California 94035

NEWELL TRASK
U. S. Geological Survey
Reston, Virginia 22092

Submitted for Publication in the

Proceedings of: Soviet-American Conference

on Cosmochemistry of the Moon and Planets

Moscow, June 1974

ABSTRACT

The morphology and optical properties of the surface of Mercury resemble that of the Moon in remarkable detail, recording a very similar sequence of events; chemical and mineralogical similarity of the outer layers is implied. Mercury is probably a differentiated planet with an iron-rich core. Differentiation is inferred to have occurred very early. No evidence of atmospheric modification of any landform is found. Large-scale scarps and ridges unlike lunar or martian features may reflect a unique period of planetary compression near the end of heavy bombardment, perhaps related to contraction of the core.

1. INTRODUCTION

Mariner 10 acquired over 2300 television pictures in the vicinity of Mercury in order to investigate the geologic history of the planet as manifested in the morphology and optical properties of the surface. A unique surface history was suggested by the planet's earth-like density (5.5 gms/cm^3) and small size (4870 km). Instead an extraordinary similarity to the surface of the Moon has been found; the implications of this lunar-like exterior and probable earth-like interior provide critical insight into processes of planetary formation at an earlier period of time than with any planet yet investigated.

We present experimental results and consequent interpretations from preliminary study of the pictures received in the March 1974 encounter as well as quantitative analysis of about one-tenth the total. Table I summarizes the data set. High resolution photomosaics covering nearly all the lighted hemisphere of the planet were constructed from specially-processed frames of the close encounter phase (Figure 1). In regions of favorable lighting and viewing geometry the resolution is 1.5 to 2.0 km, comparable to good earth-based photography of the Moon. There are about 200 additional individual pictures of resolution ranging from 1.5 to 0.15 km. Figure 2 presents index maps showing the location and figure numbers of photographs discussed in text.

Visual examination of the pictures from a satellite search phase of the imaging experiment reveals no mercurian satellites, only stars (Figure 3). We place an upper limit of 5 km in the diameter of any hypothetical mercurian satellite with an albedo similar to that of the planet. Spatial coverage is estimated to be at least 95% complete for equatorial satellites within 30 planetary radii. Further processing is expected to improve the detection limit to about 2 km in diameter and to increase the completeness of spatial coverage.

TABLE I

SEQUENCE SUMMARY

Phase	Range (km)	Resolution (km)	Frames
INCOMING FAR ENCOUNTER -6 days to -1 day	4,500,000 - 800,000	127 - 20	716
INCOMING COLOR MOSAICKING -1 day to -3 hours	800,000 - 100,000	20 - 4	212
CLOSE-ENCOUNTER -3 hours to +3 hours	100,000 - 10,000	4 - 0.15	548
OUTGOING COLOR MOSAICKING +3 hours to +1 day	100,000 - 800,000	4 - 20	220
OUTGOING FAR ENCOUNTER +1 day to +3 days	800,000 - 2,000,000	20 - 60	112
SATELLITE SEARCH +1 day to +3 days	1,000,000 - 3,500,000	---	555
		TOTAL	2,363

The photographic coverage provided by Mariner 10 is so extensive that a mercurian surface coordinate system and control net is necessary. Coordinates of features (control points) on Mercury are being computed photogrammetrically by methods similar to those developed for use with Mars (Davies, 1972, 1973; Davies and Arthur, 1973). As of May, 635 measurements of 151 points on 45 pictures have been incorporated in the control system. A series of maps is planned as the cartographic base for future systematic geologic mapping.

In the Mariner 10 coordinate system the axis is assumed always to be normal to the orbital plane of Mercury (0° obliquity). The crater Hun Kal (Figure 4), about 1-1/2 km in diameter, has been chosen to define the system of longitudes; the 20° meridian passes through its center at latitude about 0.4° south (Figure 3). Thus, the 20° meridian defines the longitude on Mercury in the same way that the 0° meridian (Greenwich) does on Earth.*

---

*The International Astronomical Union in 1970 defined the origin of planetographic longitudes as the meridian containing the subsolar point at the first perihelion passage of 1950 (JD 2433292.63) and recommended the use of a rotational period of 58.6462 days. This definition is adequate for astronomical use; however, it does not tie the meridians directly to surface features since intermediate steps of spacecraft trajectory, camera pointing angles, etc., must be known precisely. Thus, it was necessary to redefine the system of longitudes relative to a small, conspicuous crater (Hun Kal) so that the coordinate system is rigidly fixed to the surface features; a similar crater-definition of longitudes was adopted for Mars in 1972 following the Mariner 9 mission. This Mariner 10 Mercury coordinate system can be related to the IAU system through the control net computations, which currently give a value of 359.92 for the longitude of the prime meridian of the IAU system.

II. SURFACE OPTICAL PROPERTIES

Earthbased observations indicate that the integral optical properties of Mercury are closely similar to the global average of the Moon (de Vaucouleurs, 1964; Dollfus and Aueiere, 1974; Hameen-Anttila, et al. 1970; Harris, 1961; Irvine, et al. 1968; Lyot, 1929; McCord and Adams, 1972). The average microrelief and surface composition of the two objects, therefore, have been inferred to be similar. Mariner 10 provided an opportunity to determine whether this similarity extends to regional variations in optical properties such as the highland/maria dichotomy of the Moon. In addition to a comprehensive preflight photometric and geometric calibration, extensive photography of Earth and Moon was carried out from Mariner 10 shortly after launch to permit direct comparison between Mercury and the Moon.

The relative brightness distribution in a selected image of Mercury, taken on the incoming leg of the trajectory, is virtually identical to similar plots of lunar data made both from Mariner 10 and earthbased observations at similar phase angle. Also, the ultraviolet plane polarization of Mercury in the phase angle range 80-100° is indistinguishable from that of the Moon down to a scale of about 50 km at least. Evidently the mercurian surface observed by Mariner 10 is everywhere covered with a fine-grained material analogous to the lunar regolith.

The normal albedos,* corrected to a wavelength of .55 μ were measured for 33 representative areas. Their locations are shown in Figure 5 and the results of the measurements are summarized in Table II. Relative accuracy is estimated to be 10-15%; absolute errors may be somewhat larger. Crater Kuiper (Number 1, Figure 4; also see Figures 1 and 2) is one of the brightest areas on the visible hemisphere of Mercury with a normal albedo of 0.25. Both the interior of the Caloris Basin and of the smooth plains outside the basin rim have albedos of 0.12. Heavily cratered terrain has approximately the same average albedo as do the lunar highlands, and the smooth plains of Mercury are significantly darker. However, Mercury's appearance is more bland than that of the Moon. There is less contrast between adjacent units; albedo boundaries between light and dark regions are apparently less distinct on Mercury than on the Moon, as is illustrated in Figure 6.

---

*The normal albedo is defined as the ratio, at zero phase angle, of the brightness of an area to the brightness of a Lambert surface viewed from the normal. The minimum phase angle at which Mariner 10 observed Mercury was about 75°. The normal albedo of features on Mercury was estimated by interpolation using the lunar photometric phase function. The lunar observations made by Mariner 10 shortly after launch were used to confirm the prelaunch calibration. Normal albedos of several lunar regions were measured and compared with the Pohn-Wildey lunar albedo map (Pohn and Wildey, 1970) and with the measurements of Dollfus et al. (1971), Bowell et al. (1972), and Dollfus and Auelere (1974).

TABLE II

NORMAL ALBEDOS

Lunar Features	Earth-based	Mariner 10
M. Crisium	.085	.10
M. Serenitatis	.09	.10
Highlands between Crisium and Serenitatis	.16	.17
Brightest Crater	.23	
Integrated disk	.125	
Mercurian Features		
Bright craters, rays (1,6,7,11,14,22,23,28, 29,30,31)		.19 - .25
Heavily cratered terrain and textured plains (4,9,10,12,13)		.11 - .19
Flat-floored craters (3,2)		.10, .13
Smooth plains (15,16,17,18,20,26,27,33)		.08 - .12
Integrated disk	.125	

Regional scale color variations were investigated by forming ratios of pictures taken in the orange (OR) filter to those taken in the UV filter (see Figure 7 for spectral responses of each filter). No pronounced regional color differences were apparent, the maximum dispersion in the OR/UV ratio being approximately ± 5%. In particular, no areas with nearly flat reflection spectra and high plane polarization, which might indicate the presence of significant amounts of metallic Fe on the surface, were noted. Like the Moon, brighter areas are generally redder than average, although many exceptions to this rule occur. For example, crater Kuiper (lat. -11°, long. 31°) is redder, but the bright crater near latitude 36°, longitude 127° is bluer. The 440-km diameter basin at latitude -15°, longitude 165° has a light, reddish interior surrounded by a darker, bluish border. The interior plains of Caloris Basin are also redder than average. Such faint color differences very likely correspond to compositional differences in the surface materials on Mercury similar to those found on the Moon within individual mare or associated with fresh craters. Thus, a surprising similarity to the Moon is exhibited in regional color variations as well as albedo variations. Mercury does indeed resemble the Moon on a regional basis as well as global. Regional differences in optical properties on the Moon generally reflect chemical and mineralogical variations within the overall iron silicate composition of surface material. Grossly similar variations are suggested for the surface of Mercury by the Mariner 10 picture data.

III. CRATERS AND CIRCULAR BASINS

Craters are the predominant landform on Mercury. The areal density differs from one part of the surface to another (Figure 8), similar to the difference between the highlands and maria on the Moon. With increasing size, craters grade into basins--circular structures with an arbitrary lower limit, for purposes of this paper, of 200 m diameter. The craters are morphologically similar to lunar craters of the same size and evidence the same stages of degradation as their lunar counterparts. This indicates to us that similar formation and erosive processes have been active, especially meteoroid impact.

Craters smaller than ~10 km diameter grade from shallow, barely discernible depressions to bowl-shaped cavities exhibiting well-developed raised rims, ejecta deposits, secondary crater fields, and, around some craters, ray systems contrasting in albedo with the surrounding surface. Larger degraded craters, which have lost their ejecta deposits and secondary crater fields and have no prominent raised rims, are typically shallow, flat floored, and sometimes are filled with plains materials. Fresher and presumably younger features commonly exhibit essentially flat floors and terracing on the interior walls; central peaks or ringed complexes are prevalent. The continuous ejecta deposits of the larger craters do not extend as far from the crater rim as for otherwise similar lunar craters. Similarly, the radial distance to the position of maximum areal density of secondary craters is closer to the rim of mercurian craters, and preliminary depth-diameter measurements for 131 craters ranging from 3 to 200 km suggest that mercurian craters are significantly shallower than similar-sized lunar craters. All three differences are consistent with Mercury's greater gravitational acceleration, which can reduce the ballistic range of

Crater size-frequency distributions were obtained using the techniques and procedures described by Greeley and Gault (1970), as a basis for determining the relative ages of major physiographic provinces and several selected surface units (Table III and Figure 9). Areas in which the crater counts were made are indicated in Figure 5. The heavily cratered terrain observed prior to encounter is not only grossly similar in general appearance to the lunar highlands but also has a crater frequency distribution (Figure 9) essentially identical to that of the southern highlands on the nearside of the Moon. Both surfaces have attained equilibrium or steady state conditions (Gault, 1970; Shoemaker et al., 1970) with craters as large as at least 100 km in diameter; landforms there have survived since the end of intense bombardment by small planetesimals.

Table IV lists all basins larger than 200 km diameter within the areas of favorable lighting areas outlined in Figure 8. The basins show a variety of morphologies depending on their size, relative age, and degree of flooding by plains materials. The smaller basins tend to have two well-preserved rings with the diameter of the outer ring close to twice that of the inner (Figure 10). Both rings are of relatively low relief. Radar measurements give a height of 1.5 km relative to the basin floor for the outer ring of basin 5 (Goldsten and Zohar, 1974). In some basins, the inner ring is partially covered with plains materials and the area between the two rings contains irregular hills. Exterior to the outer ring, radial structures dominate, consisting of hills, valleys, gouges, and strings of craters. Secondary craters and gouges occur as close as 1/4 crater diameter to the outer ring and extend outward in a continuous field to 1 crater diameter in the freshest examples (Figure 10).

TABLE III

CRATER UNITS

Surface Location (Figure 5)	Number of Craters Counted	Area (km^2)
1) Heavily cratered (area A)	1538	4.28×10^6
2) Plains (area B)	107	2.33×10^4
3) Plains (area C)	56	1.14×10^4
4) Caloris Basin (area D)	95 261	4.04×10^5 1.23×10^5
5) Plains east of Caloris Basin (area E)	416 2432	8.50×10^5 3.11×10^4
6) Plains (area F)	429	6.33×10^3

TABLE IV

CIRCULAR BASINS OBSERVED IN MARINER 10 PICTURES

(March 1974 Encounter)

Feature Number	Latitude	Longitude	Diameter
1) Caloris	+30	190	1300 km
2)	-15	165	440
3)	+85	30?	350
4)	-2	45	385
5)	0	37	330
6)	+31	159	410
7)	+43	158	240
8)	-18	52	220
9)	-77	100	200
10)	+10	190	220
11)	+52	133	200
12)	-64	20	250
13)	-16	13	240
14)	-45	178	430
15)	+48	150	310
16)	+27	163	240
17)	+21	19	230

The Caloris Basin, the largest structural feature apparent in the Mariner 10 pictures, is similar in appearance and size to the lunar Imbrium Basin and undoubtedly originated by impact of a body at least tens of kilometers in diameter (Figure 11). The basin is bounded by a ring of mountains about 1300 km in diameter which forms an irregular scarp averaging around 2 km in height above the basin floor (see cover). Between about 23 and 30° N latitude, the scarp is very subdued and appears to be mantled by plains material. In the northeastern part of the basin, a weak outer scarp occurs at a distance of about 150 km beyond the main scarp. Between these two scarps is a terrain characterized by relatively smooth hills or domes similar in appearance to the terrain basinward of the Rook Mountains in the lunar Orientale Basin. Surrounding the main scarp and extending outward for at least one basin diameter is a radial system of linear hills which is best developed northeast of the basin. The radial system is only weakly developed in the terrain between the two scarps; its main development begins beyond the outer scarp in this area. This radial system of hills is embayed by smooth plains material which completely surrounds at least the visible eastern portion of the basin.

Stuart-Alexander and Howard (1970) counted 24 well-defined basins 300 km and larger on the Moon. In contrast, we have observed 8 basins larger than 300 km over approximately 1/3 the surface of Mercury, suggesting about the same total of 24 for a body with a surface area twice that of the Moon. However, we observe no basins in the size range 500 to 1300 km; the total for the Moon in this size range is 5 (Stuart-Alexander and Howard, 1970). The relative deficiency of large basins on the surface of Mercury so far viewed probably has affected the regional appearance of the planet when compared to the Moon. Ejecta blankets and

secondary craters are observable around virtually all basins which are not flooded by plains materials exterior to the outer ring. Destruction of these features by subsequent basins larger than 500 km apparently has not occurred on the observed surface of Mercury to the same degree as on the Moon (Howard et al., 1974).

IV. PLAINS

The floors of many basins and craters, and the surfaces around several large basins are level, except for scarps and ridges. These surfaces are relatively free of craters above 10 km diameter and are referred to as plains; they are obviously younger than the surrounding heavily cratered terrain. The mercurian plains seen in Mariner 10 pictures strongly resemble the lunar maria. It is important to establish whether a similar volcanic origin also can be inferred for at least some of the mercurian plains. In the following we review the morphological evidence which bears on the origin of the plains.

The general distribution of plains materials seen by Mariner 10 is plotted in Figure 8. Many craters in the diameter range 100-200 km are filled with plains materials, but others are not, including some that appear to be as old as those that are filled. The plains materials on Mercury fill all of the basins on the planet but to different degrees. Particularly important is the difference between the 350-km north polar basin (Number 3, Table IV), which is filled and surrounded by a broad belt of plains and a basin of identical size at 45° South (Number 14, Table IV) which contains only a restricted area of plains on its floor. These relations are more easily explained if the plains formed in episodes of volcanism following formation of most of the basins rather than as impact melts at the time of each cratering event.

Plains material containing the ridges and scarps surrounds the Caloris Basin in an arcuate band from 1000 to 1500 km wide (Figure 8). Radar studies (Goldstein and Zohar, 1974) suggest that the band continues around at least the southwest rim of the basin some 1000 - 2000 km on the side not illuminated at the time of the Mariner 10 flyby. In places, hills of more rugged material project through these plains suggesting that the material is relatively thin. The Caloris Basin itself is filled to within about 2 km of the highest peaks in the surrounding mountains.

The plains inside the Caloris Basin contain numerous ridges and are intensely fractured (cover). The ridges range from 1.5 to 13 km in width, have heights of about 300 m and lengths in excess of 300 km and are grossly similar to lunar mare ridges. The extent and complexity of ridges and associated fracturing on the plains inside the Caloris Basin is greater than on lunar maria. Fractures are closely spaced with some forming a polygonal pattern; others are almost sinuous, although unlike lunar sinuous rilles in detailed planimetric outline. They range in width from 6 km down to the resolution of the best photography of the basin floor (~ 700 meters). The widest fractures are flat-floored and graben-like. Fractures transect, are parallel to, and even occur along the tops of ridges. Directions of fractures tend to mimic the trend of the ridges, suggesting that the structures are related. The fracture pattern seems consistent with gentle subsidence of the central part of the basin floor following emplacement of the plains.

A typical high resolution view of two areas of plains and their surroundings (Figure 12) shows that the rims of the enclosing craters have been battered by abundant craters not present on the younger, smooth floors. In another area

(Figure 13) a series of filled craters show progressively greater structural disruption of their rims indicating a lapse of time between crater formation and filling by plains materials. These plains materials are unaffected structurally and appear to be about the same age in each depression. Some plains materials fills craters and basins which are younger than the broad belt of plains around the Caloris Basin (Figure 9) and so are younger than parts of that belt.

Crater populations for plains within Caloris Basin and the surrounding plains units east of Caloris (Figure 9) are indistinguishable, indicating that the emplacement ages of the two surfaces are similar.

The crater distribution for these mercurian plains (Figure 9) is almost the same as that obtained for the Apollo 14 landing site (Gault and Greeley, 1974) and the population of 1 km diameter mercurian craters is a factor of 10 greater than the Apollo 12 site which yielded rocks with the youngest crystallization ages from the Moon. However, any attempt to assess the age of the mercurian plains by comparison of crater frequencies with the lunar maria must take into account differences in cratering mechanics between the two bodies as well as possibly different fluxes of post-accretion impacting bodies.* The Caloris Basin

*Mercury's gravitational acceleration is greater than that of the Moon by a factor 2.2. This difference will tend to inhibit crater size. On the other hand, impact velocities at the surface of Mercury should be greater than for the lunar case if the impacting bodies are from the same source, making larger craters for impacting objects of the same mass. Although these two factors are compensating, effects of velocity probably dominate. Mercurian craters produced by a given impacting mass plausibly could be two to three times larger than

(Continued)

and other plains units exhibit production crater populations (Gault, 1970) in contrast to the heavily cratered terrain (Figure 9) which is in a state of crater saturation.

Patches of plains materials on the floors of craters and basins over the rest of Mercury are indistinguishable in age or morphology from the plains concentric to and inside Caloris. Some of these smaller tracts of plains materials could perhaps be impact melt from nearby craters or basins, although for many there is no well-defined source crater (Figure 12). Although we have observed no direct evidence of volcanism such as cones, domes or flow fronts, we emphasize that such features are best observed under very low Sun illumination and we see only a single narrow band on the planet with such lighting.

The origin of the plains material is of key importance because the occurrence of widespread volcanism in combination with its great bulk density would strongly imply that Mercury is differentiated. The volumes and areal distribution of the plains materials are the main arguments in favor of a volcanic origin as opposed to an origin as solidified impact melt or debris flows. The plains materials filling the Caloris and north polar basins cannot be the direct result of the impact which formed these basins because their volume is very close to the volume of material that was excavated during the cratering event. Subsequent filling by fluid material is required.

(Continued)
their lunar counterparts. This difference would be manifested as an increased number of craters of any given size for the same accumulated fluxes at both bodies. Thus the similarity between the frequency distributions for the Caloris plains units and Apollo 14 site is only apparent and the implied ages would be different even if the impact flux histories could be assumed equal.

The structure and morphology of the Caloris Basin, immediately after it formed, probably resembled those of the Orientale Basin on the Moon. The latter has numerous hummocky fissured areas on the floor and some smooth plains both of which probably formed from impact melt as well as relatively small dark plains (maria) believed to be of genuine volcanic origin. However, the volume of the Orientale melt material is insignificant compared to volume of its impact cavity out to its outermost rim. Similarly, the plains materials concentrically surrounding the Caloris and north polar basins involve enormous volumes of melted material--more analogous to the mare flooding of Oscanus Procellarum adjacent to Mare Imbrium than to the light plains materials (sometimes called Cayley Formation) containing impact breccias which concentrically surround the Imbrium Basin in disconnected patches (Wilhelms and McCauley, 1971).

The plains-filled basins conceivably may be the site of gravity anomalies similar to the lunar mascons. O'Leary (1968) speculated that a non-uniform distribution of regional gravity anomalies might provide the gravitational inhomogeneity required to keep Mercury in its 3/2 spin resonant period. The location of the large Caloris Basin near the mercurian "hot" pole, i.e., near the equatorial region, preferentially pointed toward the Sun at perihelion is suggestive in this regard. However, detailed measurements of the non-spherical portion of Mercury's gravity field (probably with an orbiting spacecraft) will be required to verify if Caloris and other circular basins on Mercury actually exhibit mascon-like gravity anomalies.

V. UNIQUE SURFACE FEATURES

Large scarps of great linear extent that transect both craters and inter-crater areas appear to be unique features of Mercury. Several of the largest of these features are shown in Figure 8. These features are best seen on the heavily cratered incoming side of Mercury. Preliminary shadow measurements indicate that several of the scarps may attain heights of 3 km or more. They generally have sinuous outlines with slightly lobate fronts and commonly attain lengths well over 500 km (Figure 14). The scarps face in various directions, although east-facing scarps appear to be more frequent in the incoming view. Often large craters interrupt their paths, suggesting that at least some of the scarps were formed during the final stages of intense bombardment of the surface. The lobate form of the scarps, and their crater transection relation, suggests that they may be thrust or reverse faults caused by compressive stresses. If this interpretation is correct, then Mercury is the first planet other than Earth to show evidence for global compressive stresses on this scale. Such compressive deformation was evidently significant during the later phases of heavy bombardment, if not earlier.

A peculiar terrain of hills and lineations (Figure 12a, b), confined to a semi-elliptical area of at least 500,000 km^2, is centered at latitude 20° S and longitude 20°, approximately antipodal to the Caloris Basin. Because the terrain extends into the terminator, the areal extent may be considerably greater. This terrain is grossly similar to the hilly and furrowed terrain northwest of the lunar Mare Humorum (Wilhelms and McCauley, 1971). The hills are generally wider than in the lunar example; whether there are other significant differences is not clear without additional picture analysis. The hilly and lineated terrain

on Mercury includes craters whose rims have been broken up into hills and depressions. Some craters are more strongly modified than others independent of size, suggesting that this type of terrain developed over an appreciable period of time rather than during a single catastrophic event. The extended duration yet limited geographic distribution point toward an internal origin.

The floors of many craters in the hilly and lineated terrain are almost completely filled with plains material which embays dissected crater rims and is clearly younger than the hilly and lineated terrain. Hence, the formation of this terrain appears to fall between the end of heavy bombardment and the emplacement of the plains units filling the Caloris Basin and elsewhere.

VI. PLANETARY HISTORY

The Mariner 10 picture data suggest to us that Mercury underwent a period of early heavy bombardment, including formation of huge basins, followed by the widespread volcanism represented by the plains materials. The inferred sequence of events is remarkably similar to that deduced for the Moon; we feel a strong chemical similarity to the Moon on the scale of these plains units is also indicated. But Mercury is much denser than the Moon. Therefore, Mercury must be a chemically differentiated planet; silicate outer layers probably enclose an iron-rich core.

It has been indicated for many years by ground-based radio, radar, optical and infrared measurements (Kuiper, 1970) that the materials of the uppermost centimeters to meters probably are iron-rich silicates at least grossly similar to those on the Moon (density range 3.0 - 3.3 g/cm^3). Silicate composition for at least the outer few kilometers is now indicated directly by the Mariner 10 pictures because of the similarity in albedo and morphology of the mercurian cratered terrains and plains to those of the lunar highlands and maria. Furthermore, it is likely that the resemblance to the Moon persists deeper; silicate material must extend to a considerable depth in order to have supplied the large amount of volcanic material that composes much of the extensive plains deposits. Indeed, Reynolds and Summers (1969) estimate that the iron core of terrestrial composition for a differentiated Mercury would extend outward 75 to 80% of the radius of the planet; thus the silicate outer layers would be approximately 500-600 km in thickness. Hence the most straightforward interpretation of the strong resemblence to the Moon is that Mercury is indeed Moon-like for its outer 500 km or so.*

---

*Three less likely alternative configurations of Mercury warrant brief mention:

(Continued)

(Continued)

1) Mercury has a thin skin of silicate material a few tens of kilometers thick residing on a substratum of undifferentiated rock (density ~ 5.5 g/cm^3); silicates that formed the plains have been drained laterally from over a large area; 2) The volcanic material of the plains has differentiated *in situ* into a lunar-like silicate phase and a much denser iron phase; the residual iron must then have moved downward tens if not hundreds of kilometers over a significant portion of the mercurian surface to permit adequate silicate melt to collect near the surface; 3) The silicate melt that formed the plains was "sweated" out of a uniform, undifferentiated planetary mix maintained at the eutectic temperature throughout most of its mass; the iron component is postulated to have remained solid.

Besides internal difficulties with each of these *ad hoc* possibilities, all seem poorly suited to reproduce in such detail both the small scale morphology and the broad three-dimensional form of the lunar maria. Production of extensive volcanic plains requires relatively uniform temperature and composition of source materials as well as abundant (if intermittent) flow. Whereas the first alternative might provide uniform material, it seems implausible that the flow rates for entirely horizontal transport should match closely those of the lunar maria. Furthermore, there is no evidence for widespread subsurface withdrawal that should be present for large areas surrounding the plains units on Mercury. *In situ* differentiation, the second alternative, hardly seems likely to produce a uniform melt over such large areas and extended times. A similar objection applies to the third alternative, especially because vertical transport through a porous mass over thousands of kilometers would be implied, making a mare-like flow rate of melt implausible.

What additional planetary history is evidenced by Mercury's surface? A striking feature of Mercury (and of the Moon as well) is that an ancient heavily cratered terrain has been preserved in extensive regions without major modification by either internal processes like volcanism or surface processes such as atmospheric erosion. Some of the topographic features comprising such terrain are very probably of considerable antiquity, although the precise age of mercurian heavily cratered terrain cannot be estimated with precision at this time. Analysis of samples from the heavily cratered lunar highlands has raised the possibility that the lunar heavy bombardment may have continued until four billion years ago (Tera et al., 1974) although some volcanic rocks returned from the highlands may be as old as 4.5 billion years (Albee et al., 1974). Further resolution of the history of the Moon, as well as detailed consideration of intrinsic differences in both accretion and in the flux of other solar system objects at Mercury as compared to the Moon, seems required before the terminal phases of heavy bombardment at Mercury can be assigned to a time period more precise than 4 to 4.5 billion years ago.

Survival of ancient cratered terrain sets limits on when material now composing the planet became chemically differentiated. In particular, differentiation must have been complete by the time the oldest surviving landforms were created. The complete planetary heating required for in situ differentiation of an originally homogeneous planet very likely would have significantly modified all surface topography through destructive volcanism, atmospheric effects, or even melting. Consequently, differentiation of Mercury must have occurred before the end of heavy bombardment. Since there is no evidence of any atmospheric modification to the ancient land surfaces that the planet has possessed a

substantial atmosphere since the end of heavy bombardment. The most recent impact craters on Mars, for comparison, have lost their ray systems and secondary crater chains and demonstrate the capacity for even a very thin atmosphere to modify cratered surfaces. Differentiation can, perhaps, be expected to produce an atmosphere; hence the absence of any atmospheric erosional effects suggests that differentiation substantially predicated the end of heavy bombardment.

The planetary-scale scarps and ridges, suggestive of a major episode of compression, have been recognized only in the heavily cratered terrain and not in the plains units inside or outside of the Caloris Basin. The lack of recognizably similar features on either the Moon or Mars suggests that these may record an episode peculiar to the internal constitution and evolution of Mercury. An obvious speculation is that an iron-rich interior underwent shrinkage resulting in compression of the outer layers, especially if a core were as large as suggested by Reynolds and Summers. It is conceivable that the scarps and ridges may record such an episode that persisted at least into the end of heavy bombardment but not throughout much of the rest of the history of the planet. Similarly the hilly and lineated terrain may reflect localized internal processes. While we do not offer any particular suggestion as to the nature of these processes, it may be significant that they also appear to have occurred during the terminal phases of heavy bombardment, before emplacement of the plains units.

As on the Moon, the volcanic filling of the large basins, and probably the emplacement of much of the other plains material, took place after the end of heavy bombardment. Little subsequent internal or external activity is recorded

in the observed portions of the planet. The sequence of events recorded on the surface of Mercury appears remarkably similar to that of the Moon. It is possible that not only is the relative sequence of events on the surface of Mercury similar to that of the Moon, but the incident impact flux vs. time relationships may also prove to be similar. If this proves to be the case, then absolute time scales would also be similar.

Of course, we have only viewed approximately 25% of the planet in useful viewing geometry. Previous exploration of the Moon and Mars provides ample reasons for caution in generalizing planetary history from only a limited surface sample. We cannot exclude the possibility that other kinds of volcanic processes and/or more recent internal activity are manifested on the presently unexplored parts of Mercury. Nevertheless, the constraints on differentiation and atmospheric history, and the general similarity to lunar history, remain quite valid conclusions even from the present limited surface sample.

What do these results about Mercury imply concerning the other terrestrial planets? The existence of large basins now has been recognized on the Moon, Mars and Mercury; the three bodies also exhibit striking asymmetries in their major physiographic provinces. Although not well understood, these characteristics must be acknowledged to be a rather common aspect of terrestrial planet formation. Additionally, early rather than late chemical differentiation seems supported by the Mercury results. All of these circumstances may also pertain to the formation of the Earth where direct information regarding these episodes is no longer available.

We have viewed a new world. Further study of the Mariner 10 pictures undoubtedly will contribute to a better understanding of the history of the terrestrial planets.

REFERENCES

1. A. L. Albee, A. A. Chodos, R. F. Dymek, A. J. Gancarz, D. S. Goldman, D. A. Papanastassiou and G. J. Wasserburg, Lunar Science V, Abstracts to the Fifth Lunar Sci. Conf., 3-5 (1974).
2. E. Bowell, A. Dollfus and J. E. Geake, in Proceedings Third Lunar Science Conference 3, 3103 (1972).
3. M. E. Davis, ICARUS 17 (No. 1), 116 (1972).
4. M. E. Davies, Photogrammetric Engineering 39 (No. 12), 1297 (1973).
5. M. E. Davies and D. W. G. Arthur, J. Geophys. Res. 78 (No. 20), 4355 (1973).
6. A. Dollfus, J. E. Geake and C. Titulaer, in Proceedings Second Lunar Science Conference 3, 2285 (1971).
7. A. Dollfus and M. Aueiere, (1974) (in press).
8. D. E. Gault, Radio Science 5 (No. 2), 273 (1970).
9. D. E. Gault and R. Greeley, in preparation.
10. R. Goldstein and S. Zohar, Astro. Phy. J. 79 (No. 1), 85 (1974).
11. R. Greeley and D. E. Gault, The Moon 2, 10 (1970).
12. D. Harris, in Planets and Satellites, G. Kuiper and B. Middlehurst, Eds. (University of Chicago Press, Chicago, 1961), p. 272.
13. W. K. Hartmann, Commun. Lunar and Planet. Lab. 4 (No. 65), 121 (University of Arizona, 1966).
14. K. Hemeen-Antilla and T. Pikkarainen, The Moon 1, 440 (1970).
15. K. A. Howard, D. E. Wilhelms and D. H. Scott, Reviews of Geophysics and Space Physics, in press.
16. A. J. Irvine, et al., Astron. J. 73, 807 (1968).
17. G. P. Kuiper, Lunar and Planetary Laboratory Communication 143, 165 (1970).

18. B. Lyot, Ann. Obsr. Paris 8 (No. 1) (1929).

19. T. McCord and J. Adams, Science 178, 745 (1972).

20. B. O'Leary, Nature 220, 1309 (1968).

21. H. Pohn and R. Wildey, U.S.G.S. Prof. Paper 599-E (1970).

22. R. T. Reynolds and A. L. Summers, Jour. Geo. Res. 74, 2494 (1969).

23. E. M. Shoemaker, M. H. Hait, G. A. Swann, D. L. Schleicker, G. G. Schober, R. L. Sutton, D. H. Dahlem, E. N. Goddard and A. C. Waters, in Proc. Apollo 11 Lunar Sci. Conf. 3, 2399 (1970).

24. D. E. Stewart-Alexander and K. A. Howard, ICARUS 12, 440 (1970).

25. F. Tera, D. A. Papanastassiou and G. J. Wasserburg, Earth & Planetary Science Letters 22, 1 (1974).

26. G. de Vaucouleurs, ICARUS 3, 187 (1964).

27. D. E. Wilhelms and J. F. McCauley, U. S. Geological Survey Map I-703 (1971).

FIGURE CAPTIONS

Figure 1:

Photomosaic of the incoming (right) and outgoing (left) view of Mercury with approximate coordinate system. The provisionally named features discussed in the text are indicated.

Figure 2:

Index maps showing the location and figure numbers of the photographs discussed in the text.

Figure 3:

A 36-picture satellite search sequence, taken 3.5 million km from Mercury, is shown with the background stars. The actual pointing for individual pictures is still slightly uncertain due to slight spacecraft angular motion. A satellite in a circular orbit at 30 Mercury radii would lie on the ellipse. The filled circles are three stars detected in preliminary processing of the TV pictures while the open circles are undetected stars. The visual magnitude and spectral type of the star are indicated adjacent to each circle. The detectability of the stars sets an upper limit of about 5 km in diameter for a hypothetical satellite.

Figure 4:

The 20° meridian passes through the center of the small, 1-km crater, Hun Kal, in the Mariner 10 coordinate system. Hun Kal means the number twenty in the language of the Maya Indians of Central America; the ancient Maya used a

base twenty number system. Hun Kal lies less than a degree south of the equator and defines the Mariner 10 topocentric system of longitudes on Mercury. Numerous elongate craters of probable secondary impact origin are typical of many areas on the planet.

Figure 5:

The incoming (right) and outgoing (left) mosaics of Mercury depicting the points of albedo measurement referred to in Table II. The enclosed areas indicated by letters are those used in crater counting as listed in Table III and shown in Figure 9.

Figure 6:

Mariner 10 pictures of Mercury (left) and the Moon (right) processed to appear as they would with equal illumination. The relatively lower contrast of Mercury is apparent.

Figure 7:

The integrated optics, filter and vidicon system response have been independently normalized for each spectral filter using the absolute Mercury spectrum and plotted as a function of wavelength. The effective wavelength in nanometers is shown by each filter name (UV = ultraviolet, MUV = minus ultraviolet).

Figure 8:

Sketch map showing major physiographic provinces on Mercury within approximately 60° of the terminator on the two hemispheres viewed by Mariner 10 and shown in Figures 1 and 5. The rim crests of basins, arbitrarily chosen as 200 km or larger, are shown by a dash-dot symbol and keyed by number to Table IV. The more prominent craters larger than 100 km are also shown. Ejecta and secondary craters around craters and basins are indicated by radial lines.

Figure 9:

Crater size-frequency distributions (for major physiographic provinces and selected areas shown in Figure 5) are expressed as the cumulative number of craters larger than a given diameter and compared with percentages of saturation as defined by Gault (1970). Equilibrium conditions (i.e., rate of crater production equals rate of crater destruction) are attained for crater populations at 5-10% saturation. Symbol notation:

a) ☆ Heavily cratered terrain (area A)

● Caloris Basin (area D)

\- Lunar southern highlands (Hartmann, 1966)

b) ○ Plains east of Caloris Basin (area E)

▲ Apollo 12 landing site (Gault and Greeley, 1974)

□ Apollo 14 landing site (Gault and Greeley, 1974)

c) * Plains filling crater (area B)

Δ Crater floor (area C)

■ Plains filling crater (area F)

\- Plains outside Caloris Basin (area E)

Figure 10:

Typical 200-km diameter double-ring basin (Number 11, Table IV) showing a well-developed ejecta blanket (A) and a swarm of secondary craters (B). The basin is younger than the plains material to the southwest because its secondary craters overlie the plains, in turn part of a concentric band around the Caloris Basin. This double-ringed basin is also floored by plains material. North at top.

Figure 11:

The largest basin on Mercury seen by Mariner 10 is displayed in this specially processed photomosaic. It is centered at 190° W longitude and 30° N latitude (Figure 1) and is provisionally named "Caloris" or "hot" basin for its position near one of the subsolar points when Mercury is at perihelion. The basin is bounded by a 1300-km diameter ring of mountains up to 2 km in height while the basin floor consists of intensely fractured and ridged plains.

Figure 12:

Two patches of plains materials covering the floors of older craters (A and C) whose rims are much more heavily cratered. No external source for the plains material is evident. Hypothetical impact melt from crater C should have filled both A and B, but only A is filled. A volcanic origin is indicated. The scarp (d,e) on the floor of crater A is about 400 meters high. Similar scarps have been recognized in numerous craters where they appear to be restricted to the crater floor. It is not yet clear whether they are of tectonic or volcanic origin. The blurred stripe about 1/3 the distance from the top of the picture is a processing defect. Crater A is 100 km across.

Figure 13a:

Hilly and lineated terrain whose distribution is shown in Figure 8. The rims of flat floored craters show varying degrees of structural disruption suggesting that the terrain developed over a period of time. Plains materials on the crater floors are younger than the surrounding terrain; the plains in the largest crater (170 km in diameter) have a crater number density similar to that of the plains surrounding the Caloris Basin. Area A is shown in Figure 12b.

Figure 13b:

A high resolution (400 meters) picture of the hilly and lineated terrain shown in Figure 12a. This terrain consists of numerous dissected hills (~ 0.1 to 1.8 km high) interspersed with smooth material. The southern rim (d) of the 31-km diameter crater (A) has been severely dissected, but the eastern rim (e) is largely intact. The crater rim of the smaller crater (B) is barely recognizable.

Figure 14:

A 240-km diameter basin (Number 16, Table IV) almost completely flooded by plains materials that are part of the concentric band around the Caloris Basin. The number 16 is centered in the basin, and arrows point to a ring of low unflooded hills which define the basin. The Caloris Basin lies 1300 km to the southwest. North at top.

Figure 15:

A sinuous, slightly lobate scarp (A, B) over 300 km long which transects two craters. Preliminary shadow measurements indicate a maximum height on the order of 3 km. The form, dimensions, and crater transection relations suggest that this structure (and many others of similar nature) is a thrust or reverse fault due to compressive stresses. Craters cut by scarp are 55 and 35 km across.

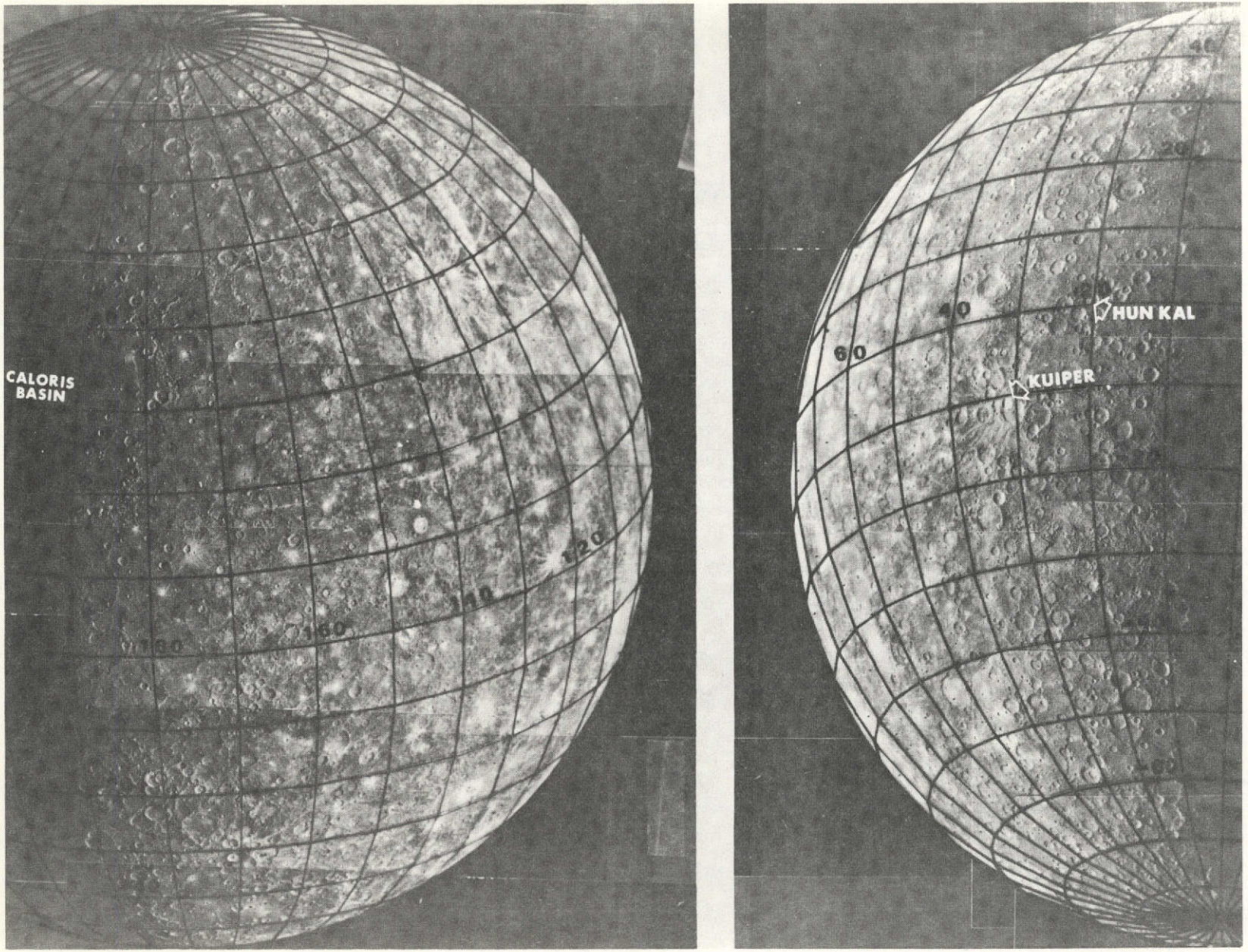
CALORIS
BASIN
120
140
160
180
HUN KAL
KUIPER
40
60

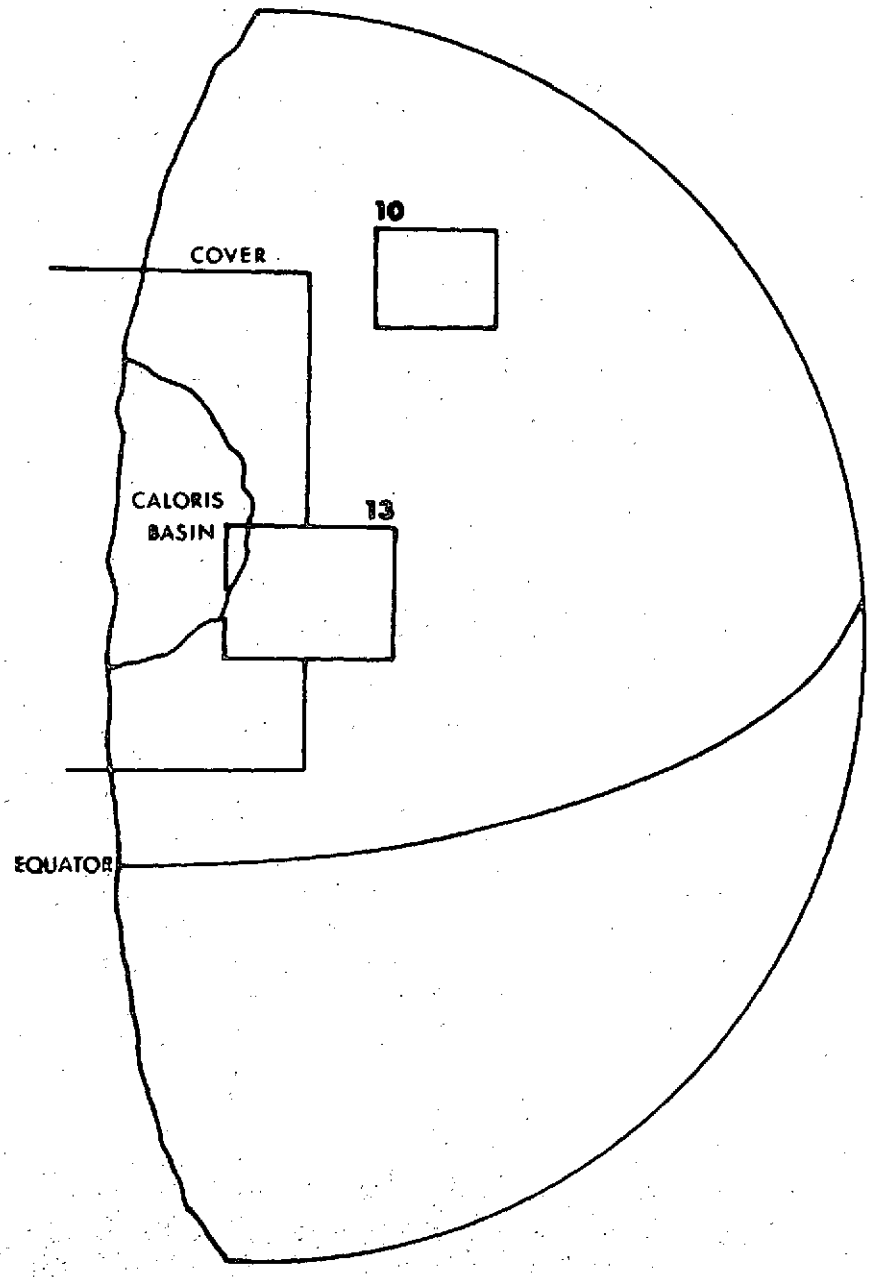

OUTGOING VIEW

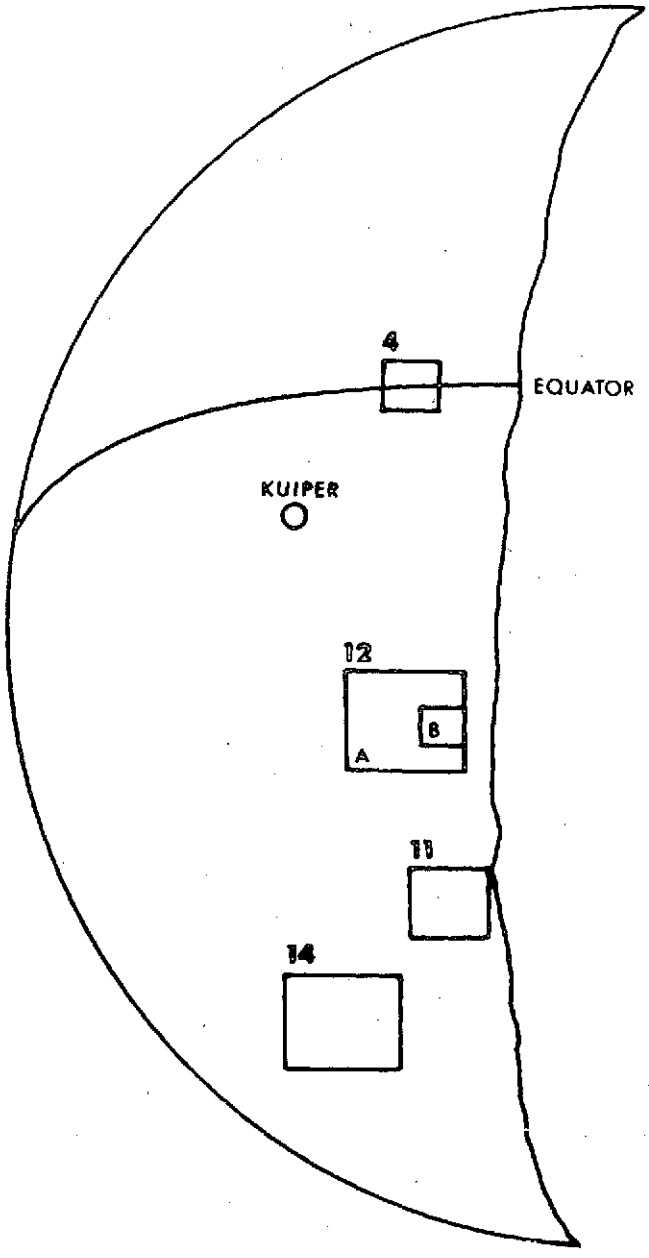

INCOMING VIEW

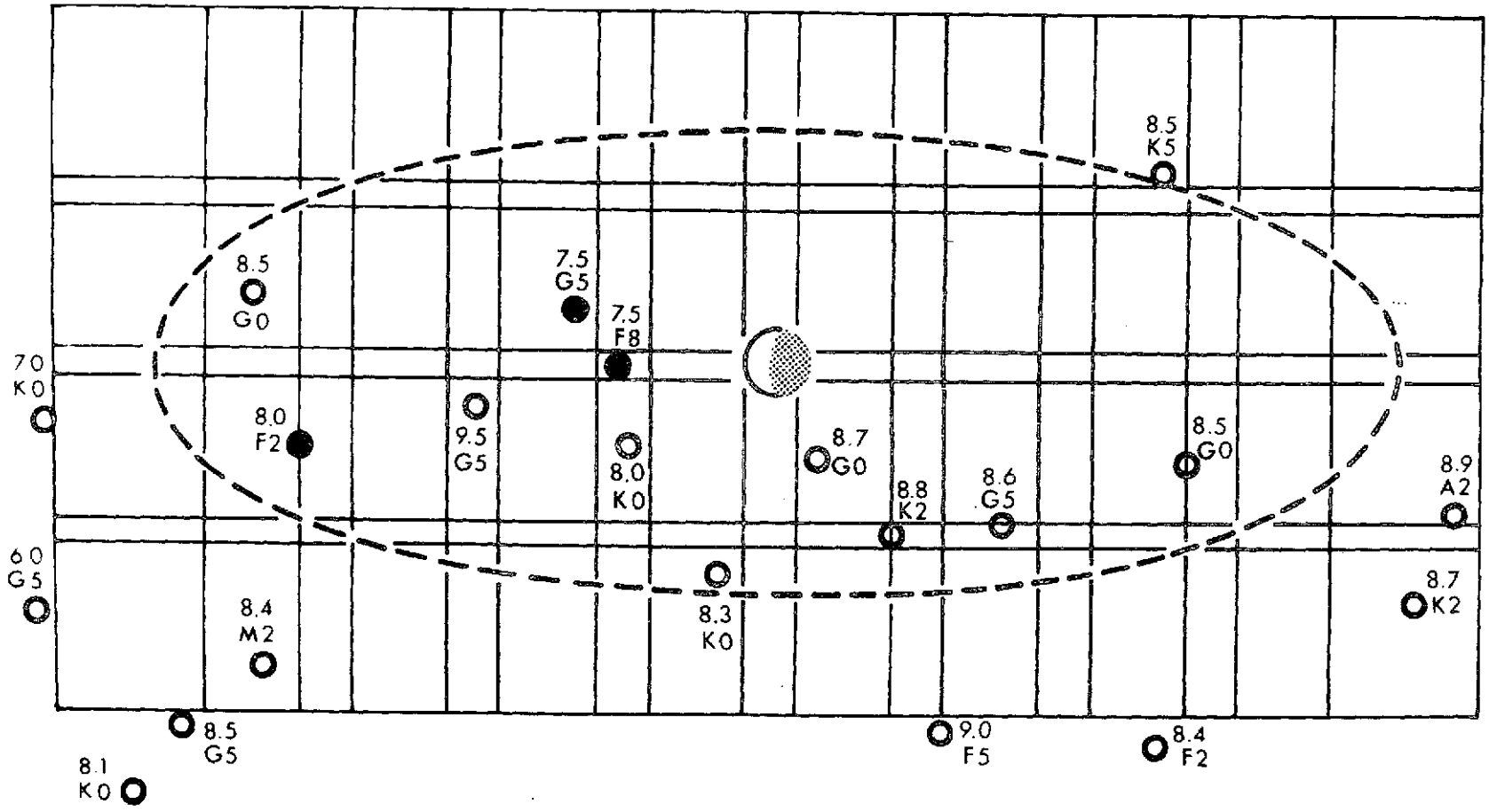
8.5
K5
8.5
G0
7.5
G5
7.5
F8
70
K0
8.0
F2
9.5
G5
8.0
K0
8.7
G0
8.8
K2
8.6
G5
8.5
G0
8.9
A2
60
G5
8.4
M2
8.3
K0
8.7
K2
8.5
G5
9.0
F5
8.4
F2
8.1
K0

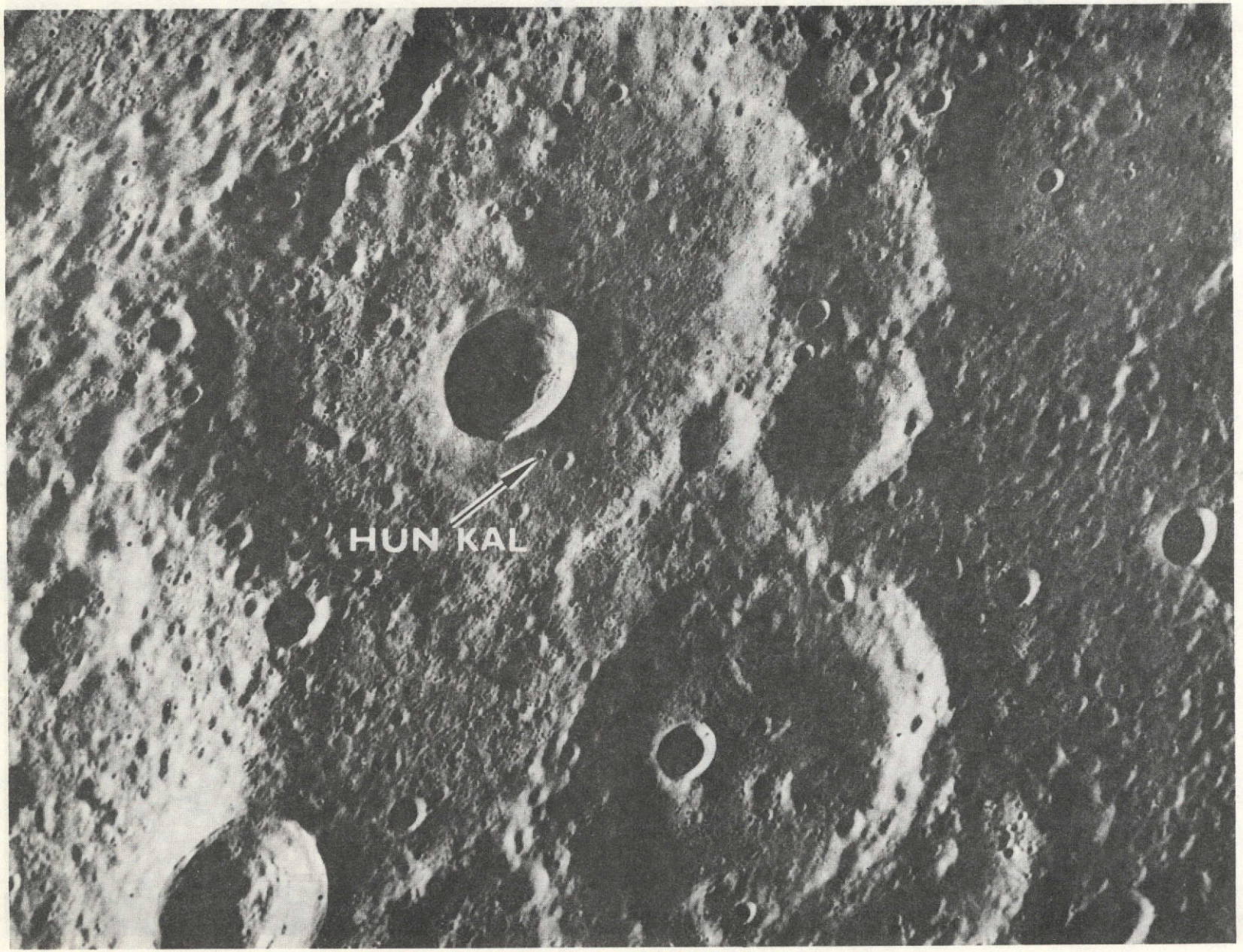
HUN KAL

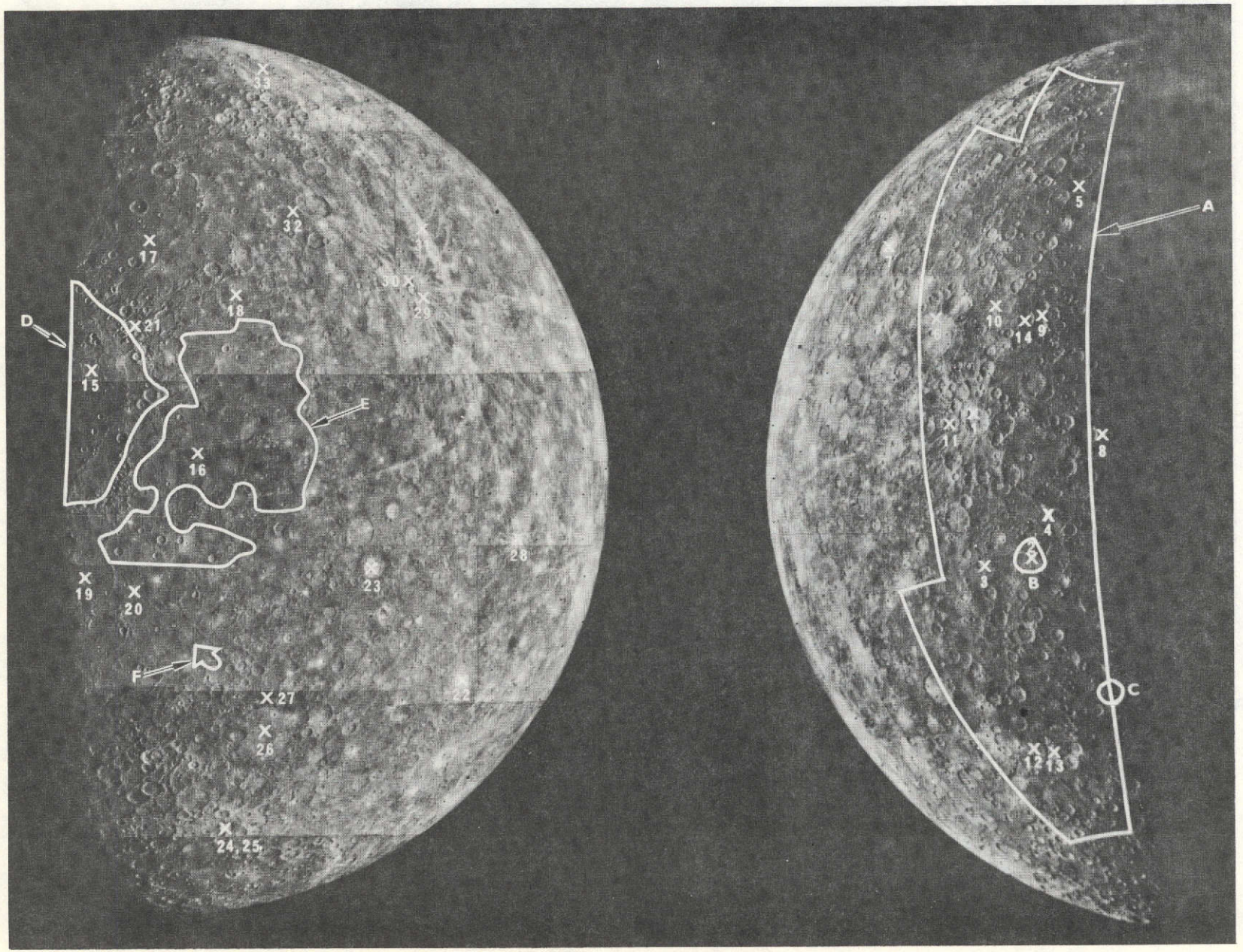
A
B
C
D
E
F
1
2
3
4
5
6
7
8
9
10
11
12
13
14
15
16
17
18
19
20
21
22
23
24, 25
26
27
28
29
30
31
32
33

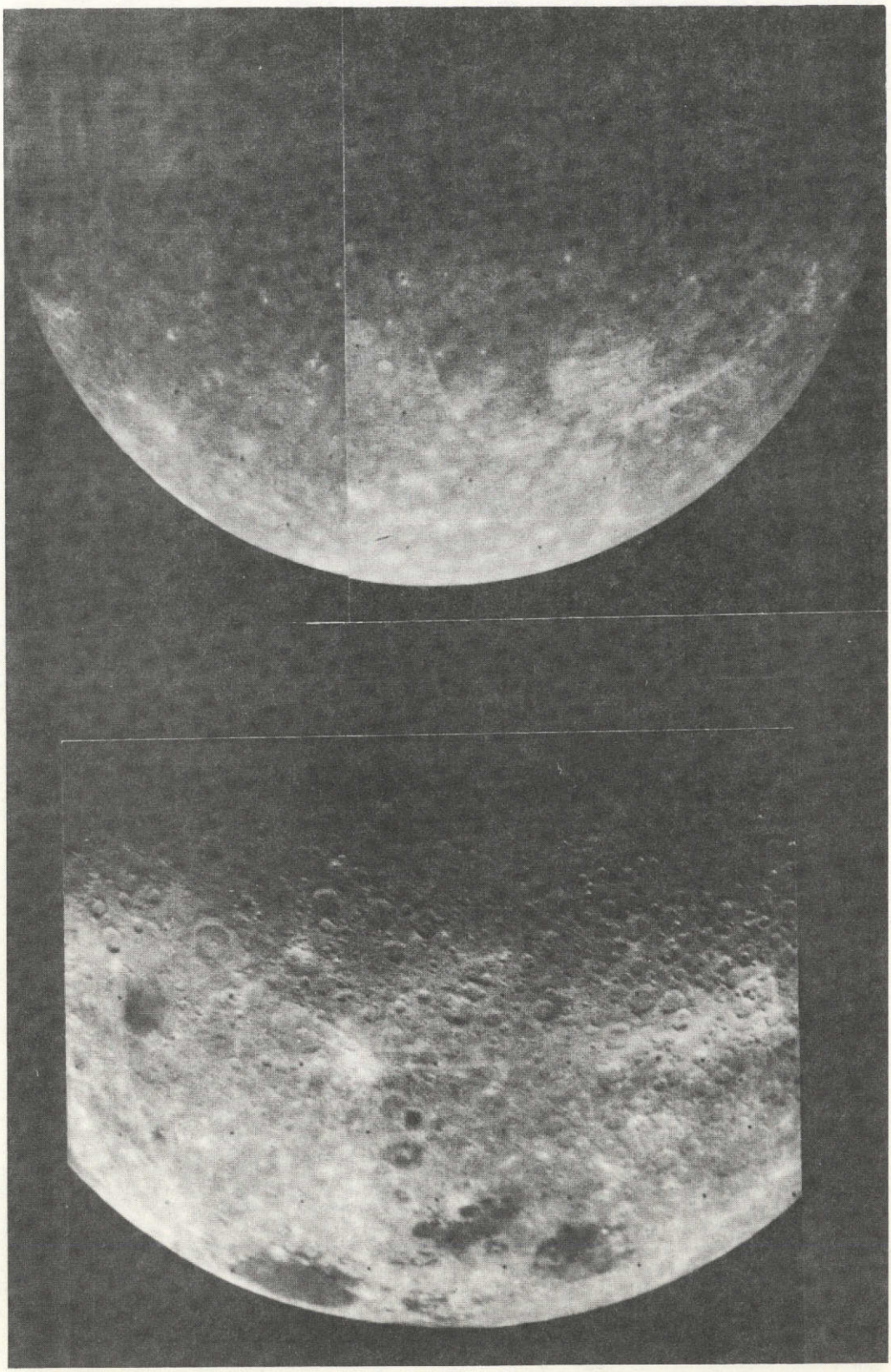

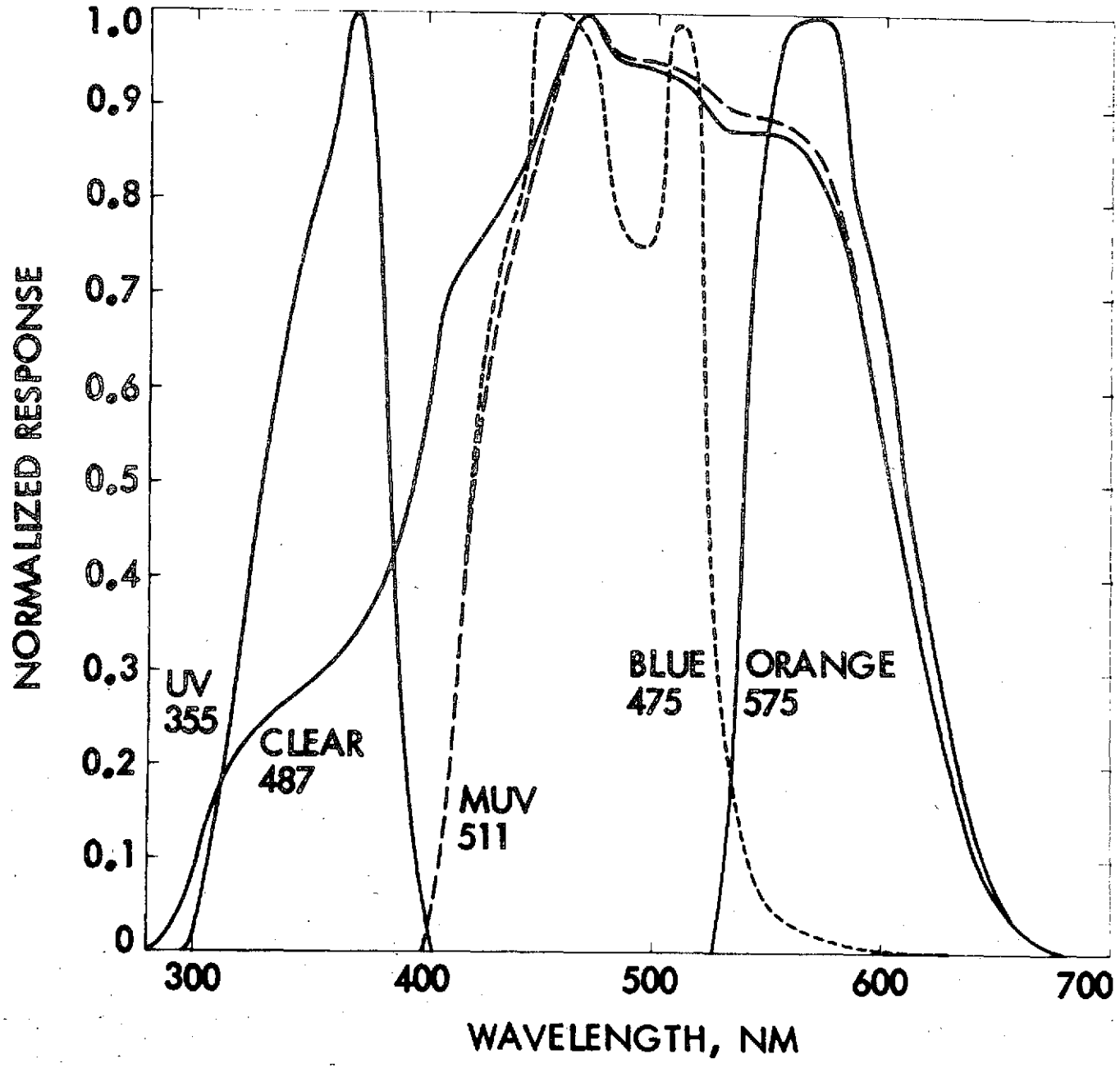
NORMALIZED RESPONSE
1.0
0.9
0.8
0.7
0.6
0.5
0.4
0.3
0.2
0.1
0
300
400
500
600
700
WAVELENGTH, NM
UV
355
CLEAR
487
MUV
511
BLUE
475
ORANGE
575

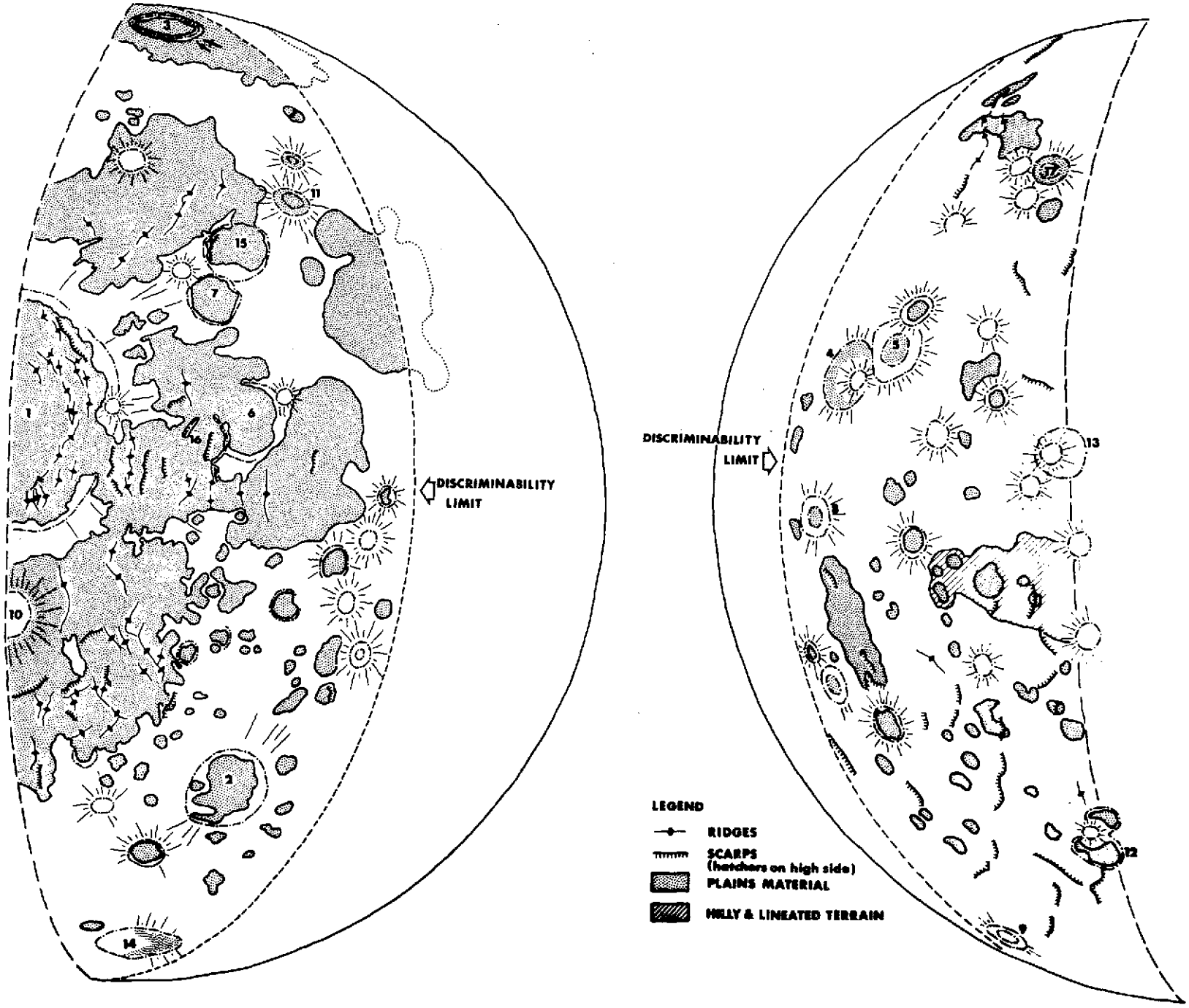
DISCRIMINABILITY LIMIT
DISCRIMINABILITY LIMIT
LEGEND
RIDGES
SCARPS (hatchers on high side)
PLAINS MATERIAL
HILLY & LINEATED TERRAIN

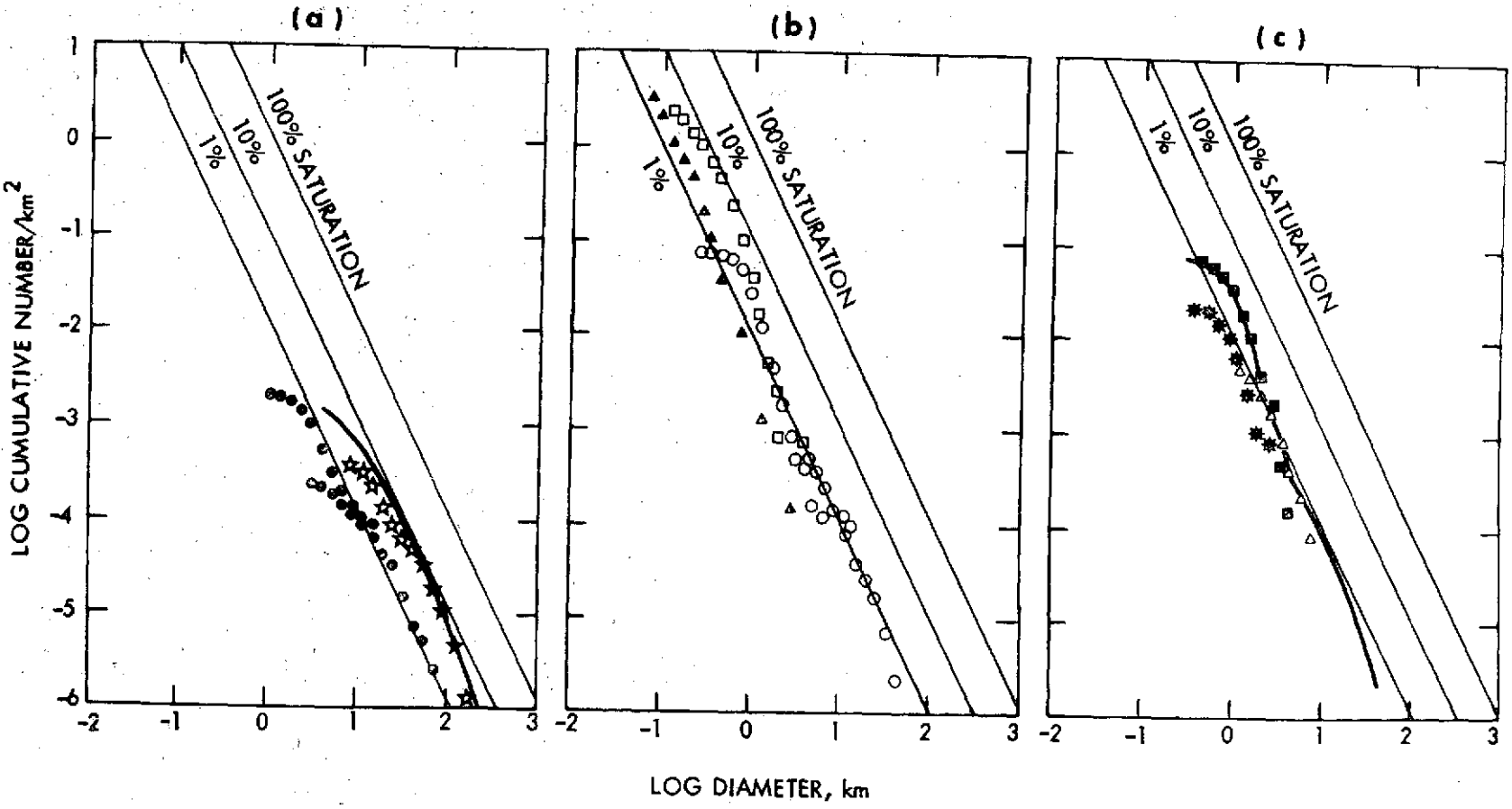
(a)
(b)
(c)
1%
10%
100% SATURATION
LOG CUMULATIVE NUMBER/km²
LOG DIAMETER, km
1
0
-1
-2
-3
-4
-5
-6
-2
-1
0
1
2
3

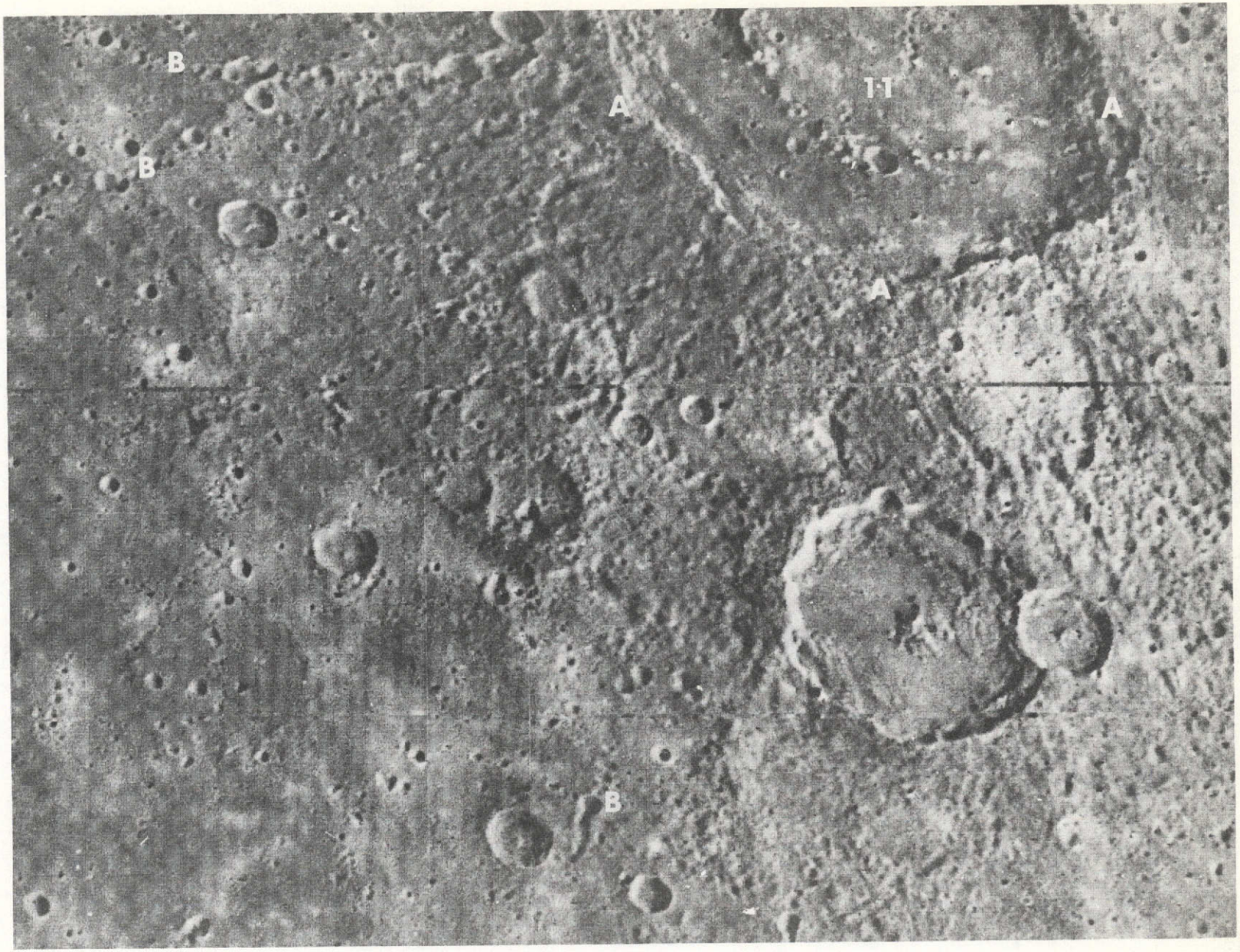
B
B
A
T1
A
A
B

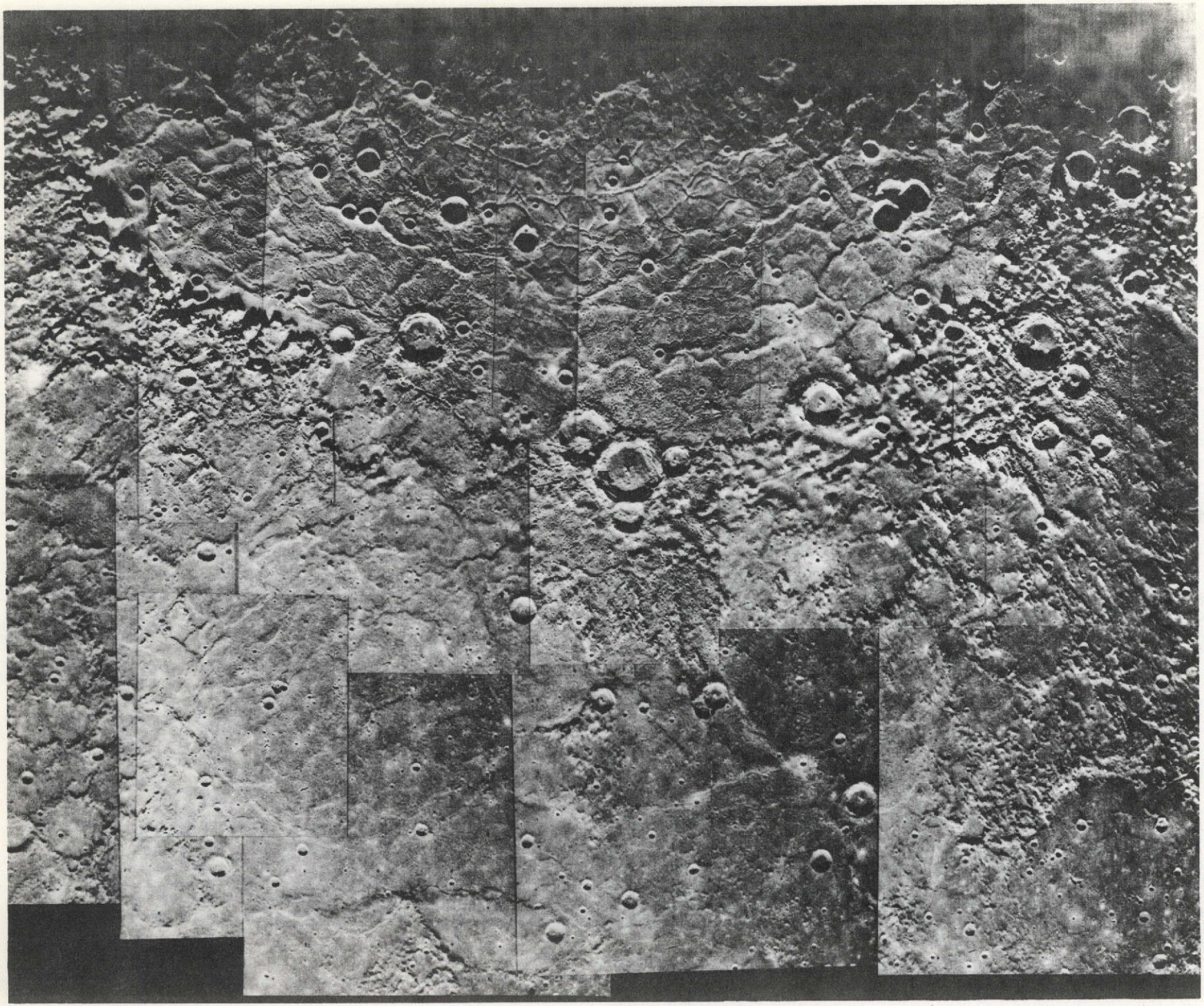

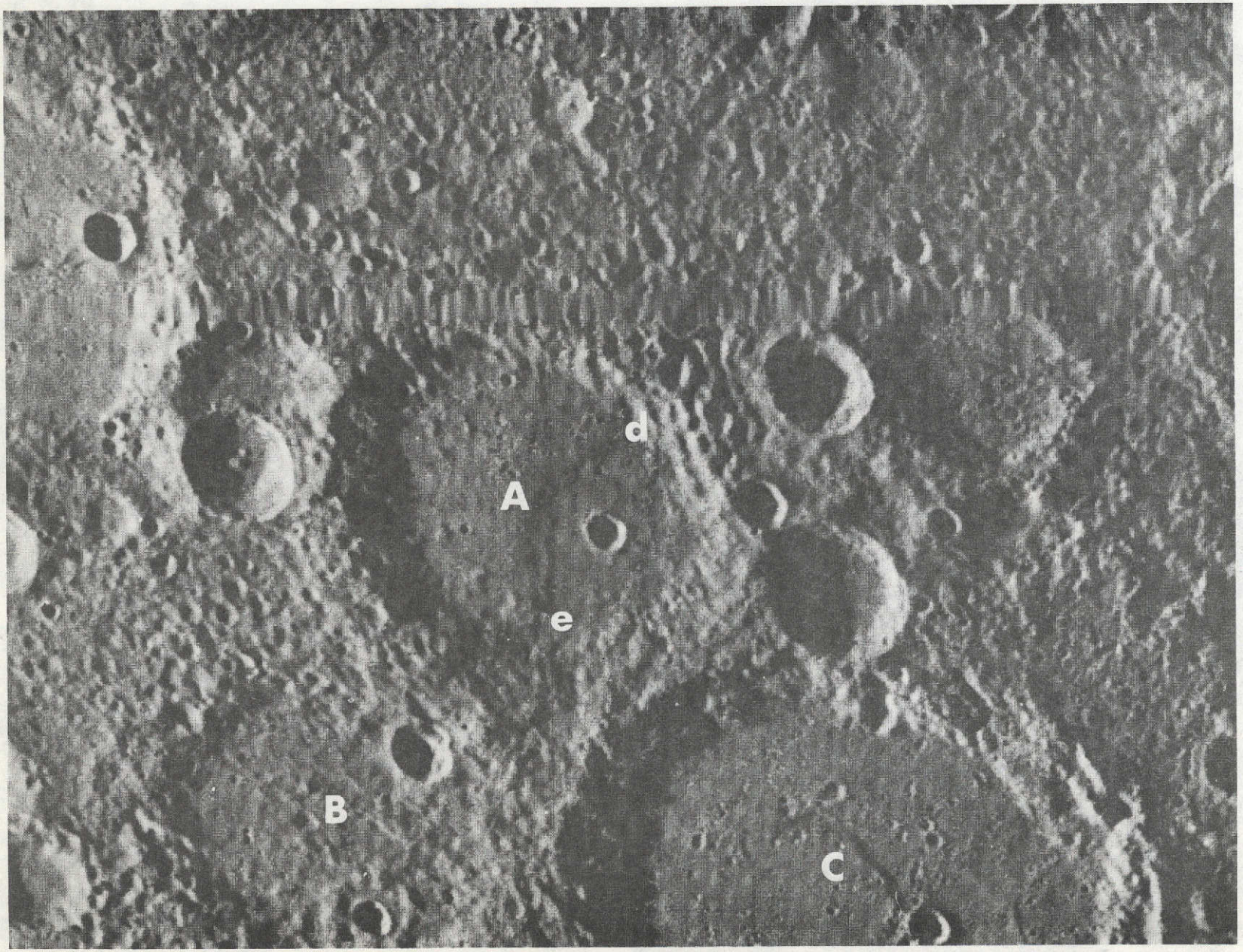
d
A
e
B
C

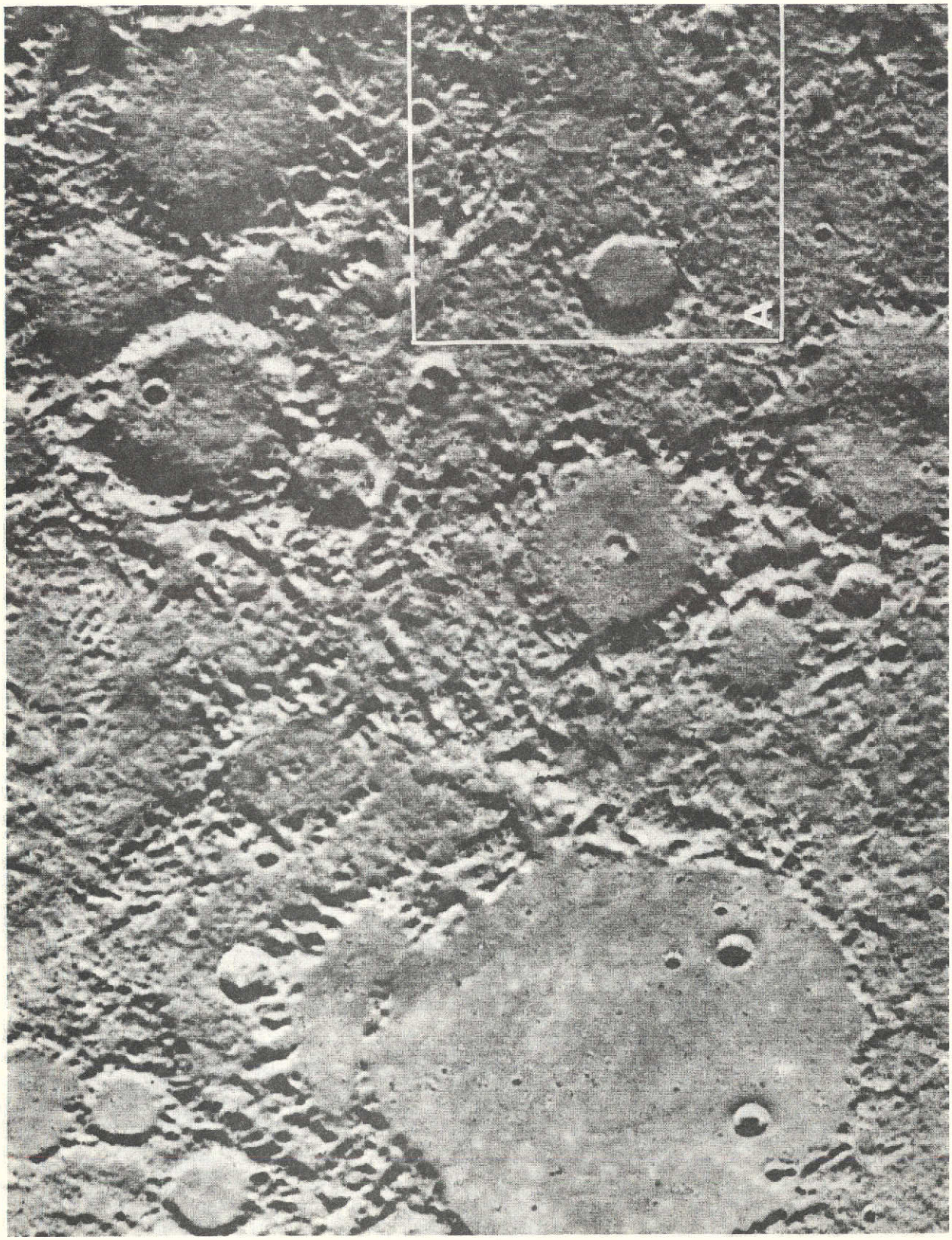
A


A
e
d
B

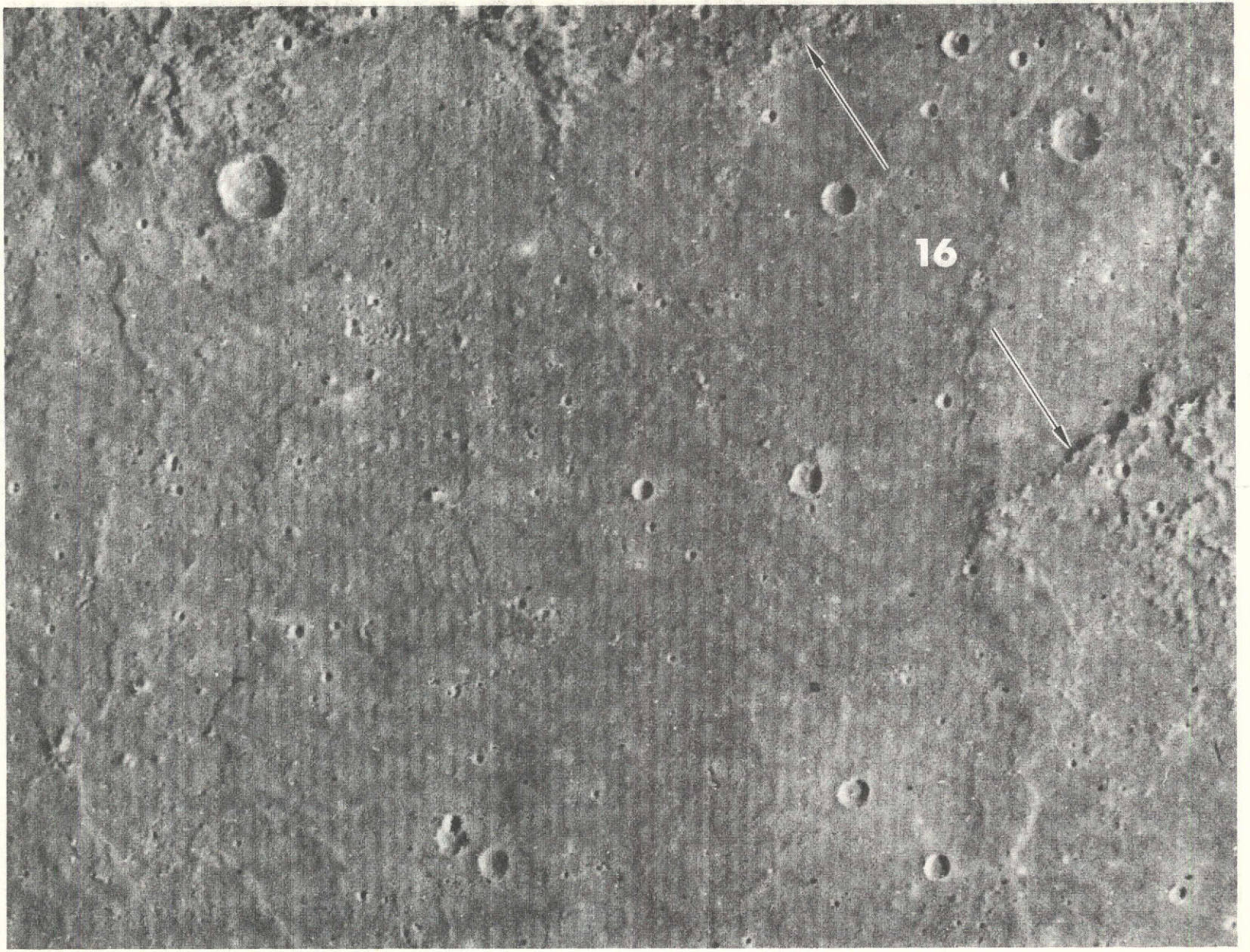
16

A
B